Solid State Science and Technology, Vol. 32, No. 1 (2024) 28-41
https://doi.org/10.66514/ssst32-1-28-41

$YBa_2Cu_3O_{7-d}$ Bulk Superconductors: Exploring the Impact of Two Synthesis Techniques on the Microstructure and Critical Temperature

Arebat Ryad Alhadei Mohamed[1], Mohd Mustafa Awang Kechik[1,], Chen Soo Kien[1], Lim Kean Pah[1], Hussien Baqiah[2], Khairul Khaizi Mohd Shariff[3], Abdul Halim Shaari[1], Yap Siew Hong[1], Nur Afiqah Binti Mohamed Indera Alim Sah[1], Muralidhar Miryala[4]*

[1]*Laboratory of Superconductor & Thin Films, Department of Physics, Faculty of Science, Universiti Putra Malaysia, 43400 UPM Serdang, Selangor, Malaysia*

[2]*Shandong Key Laboratory of Biophysics, Institute of Biophysics, Dezhou University,No. 566 University Rd. West, Dezhou, Shandong, China*

[3]*Microwave Research Institute, Universiti Teknologi MARA Shah Alam 40450, Selangor, Malaysia*

[4]*Materials for Energy and Environmental Laboratory, Superconducting Materials Shibaura Institute of Technology, 3 Chome-7-5 Toyosu, Koto Tokyo 135-8548, Japan*

* *Corresponding author; Email: mmak@upm.edu.my*

Received: 2 March 2024 / Accepted: 10 May 2024

ABSTRACT

This study explores the synthesis and characterization of high-performance $YBa_2Cu_3O_{7-\delta}$ (YBCO) superconductors via two methods: the established solid-state reaction (SSR) and a novel modified thermal decomposition (DM) technique. Notably, the DM method employs metal acetates as a single precursor for synthesis, contrasting the SSR method which utilizes oxides and carbonates as the primary metals. Two samples were prepared: YBCO-SSR and YBCO-DM. X-ray diffraction (XRD) analysis confirmed the formation of the dominant YBCO phase in both, with minor secondary phases namely, Y_2BaCuO_{5-x} (Y211) and CuO. FESEM analyses revealed marked differences in microstructure, with the DM-prepared sample exhibiting a smaller average grain size and denser packing compared to its SSR counterpart. These observations demonstrate that the modified thermal decomposition method produces an enhanced, denser, and more homogeneous microstructure for the YBCO-DM sample, which contributes to its improved superconducting properties. Moreover, the DM-prepared sample exhibited a higher superconducting transition temperature ($T_{c\text{-onset}}$) of approximately 93.24 K, compared to 91.27 K for YBCO-SSR. Additionally, the DM sample displayed a sharper transition width (ΔT_c) of 3.45 K compared with 4.57 K for YBCO-SSR. These observations suggest that the DM technique enhances the superconductivity of YBCO which is potentially attributed to the use of acetates as starting materials which can effectively dissolve yttrium, barium, and copper ions, leading to a more ordered distribution and better superconducting properties.

Keywords: *$YBa_2Cu_3O_{7-\delta}$; superconductivity; microstructure; critical temperature; modified thermal decomposition; solid-state reaction*

INTRODUCTION

Research on the $YBa_2Cu_3O_{7-\delta}$ (YBCO) ceramic compound, discovered in 1987 by Wu et al. remains a focal point in superconductivity research [1]. As a type-II superconductor, YBCO is distinguished by its critical temperature (T_c) of 92 K, making it the first material to exhibit superconducting properties above the boiling point of liquid nitrogen (77 K) [2, 3]. This breakthrough has led to an extensive research into its potential applications, especially in leveraging superconductivity for advancements in the medical and transportation sectors. In the medical industry, magnetic resonance imaging (MRI), for example, stands out as one of its most impactful applications in diagnostic medical imaging [4]. The superconducting magnet employed in MRI is an influential tool, capable of achieving magnetic field values unattainable by conventional magnets [4, 5]. Driven by the potential to unlock a new era of technological advancements, researchers delve beyond the established solid-state reaction (SSR) method, seeking alternative synthesis techniques further to optimize YBCO's properties [6-8]. The conventional solid-state reaction (SSR) method using metal oxides and carbonates is the established method, but its complexity, potential environmental drawbacks, and limitations in tailoring the material's microstructure call for alternative approaches [9, 10].

A novel modified thermal decomposition (DM) method exhibits considerable potential for revolutionizing YBCO synthesis compared to the traditional SS method. DM is a straightforward and promising approach for synthesizing YBCO superconductor powders, offering several advantages over alternative YBCO synthesis techniques [11, 12]. First, the method is simple and cost-effective, requiring only raw chemicals and a three-step heat treatment, without any catalyst [11]. Second, it is environmentally friendly, with minimal byproduct formation without any harmful catalyst [13, 14]. Third, it produces powders with small particle sizes, exceptional uniformity, and improved chemical consistency [15]. These advantages make DM a promising approach for synthesizing YBCO superconductors. To our knowledge, the DM method has not been used to synthesize YBCO bulk superconductors before. This investigation employs metal acetates as a singular starting material to synthesize bulk YBCO superconductors, aiming to enhance superconducting properties.

This study compares the efficacy of this approach with the established solid-state reaction method. The utilization of acetate in the novel modified thermal decomposition (DM) technique is based on its characteristics as a weak acid, thereby minimizing the likelihood of reactions with other chemicals in the system and thereby preserving the purity of the initial material [16]. This approach is essential in superconductor synthesis, where the pristine quality and exact stoichiometry of the starting materials critically influence the properties of the final product. Moreover, acetate enables a controlled release of metal ions during thermal decomposition, which is crucial for the formation of the YBCO superconducting phase. Furthermore, acetate improves the uniformity and distribution of metal ions, leading to the production of a high-quality YBCO superconductor. The even distribution of metal ions, resulting from acetate decomposition, plays a key role in achieving consistent superconductivity across the material [17, 18]. This uniformity is vital for creating superior superconducting materials, ensuring a consistent composition throughout and thereby boosting superconducting properties while reducing defects and grain boundaries that could impair the material's performance [18]. This modified thermal decomposition DM method can potentially revolutionize the synthesis of YBCO superconductors. The article focuses on the synthesis and characterization of pure bulk $YBa_2Cu_3O_{7-\delta}$ superconductors via established solid-state reaction SSR and novel thermal decomposition methods DM.

MATERIALS AND METHODS

Two pure $YBa_2Cu_3O_{7-\delta}$ samples were prepared: YBCO-SSR via the established solid-state reaction (SSR) and YBCO-DM using a novel modified thermal decomposition (DM) technique. For the SSR route, stoichiometric Y_2O_3, $BaCO_3$, and CuO were thoroughly mixed and ground for 2 h to homogenize the starting materials. This blend was then calcined at 910 °C for 24 h, promoting the formation of intermediate phases leading to YBCO. The resulting black solid underwent further grinding for 1 h to enhance packing density before being pressed into circular pellets (13 mm diameter and 5 mm thickness). Finally, the pellets were sintered at 980 °C for 24 h, allowing sufficient time for grain growth and phase transformation, followed by slow cooling and final annealing at 600 °C for 12 h at ambient atmosphere to optimize the formation if the crystal structure. In contrast, the DM approach employed metal acetates $Y(OOCH_3)_3.4H_2O$, $Ba(OOCCH_3)_2$, and $Cu(OOCCH_3)_2.H_2O$ as single starting materials, offering improved homogeneity and potential advantages compared to oxides. These acetates were weighed in a 1:2:3 ratio and homogeneously mixed in an alumina crucible for 15 min, eliminating the need for grinding due to their inherent fine particulate nature. Unlike the SSR route, the DM powders underwent an initial pre-calcination step at 600 °C for 30 min to decompose the acetates and remove organic residues. Following pre-calcination, the powder was ground in a mortar for 30 min and then calcined at 910 °C for 24 h in an alumina boat. The resulting black solid was then ground for 30 min, pressed into pellets, and sintered at 980 °C for 24 h under conditions similar to YBCO-SSR. Both methods aimed to achieve stoichiometric Y: Ba: Cu = 1:2:3 ratios and employed comparable thermal treatments, allowing for direct comparison of their impact on the samples characteristics. The choice of metal acetates for the DM method was motivated by their superior solubility and reactivity, potentially leading to a more homogeneous precursor mixture and facilitating the formation of a denser and more ordered YBCO microstructure.

The thermal decomposition behavior of YBCO powders was investigated using a Mettler Toledo thermogravimetric analyzer (model TGA/SDTA851e, Mettler Toledo, Zürich, Switzerland). The powders were heated to 1000 °C at a rate of 10 °C/min in a nitrogen atmosphere with a purge gas flow of 50 mL/min. Subsequently, the samples were examined using X-ray diffraction (XRD) with (XRD, Xpert Pro Panalytical Philips DY 1861 diffractometer, Phillips, Eindhoven, The Netherlands) with a CuK_α source from $2\theta = 20^\circ$ to 80°, to identify the phases and evaluate the crystal structure of the samples. Microstructural analysis was conducted using a Field-emission Scanning Electron Microscope (FESEM) along with an Energy-Dispersive X-ray spectrometer (EDX) for quantitative analyses (FESEM, FEI Nova NanoSEM 230, Thermo Fisher Scientific, Waltham, MA, USA). The four-point probe technique was used to analyze electric transport properties. The experimental setup consisted of a digital nanovoltmeter (Keithley, Model 2182A, Cleveland, OH, USA) and a DC precision power source (Keithley, Model 6221, Cleveland, OH, USA).

RESULTS AND DISCUSSION

Thermogravimetric Analysis (TGA/DTG)

Figures 1(a) and 1(b) show the thermal decomposition profiles of both samples (YBCO-SSR, YBCO-DM) as determined by thermogravimetric analysis (TGA) and differential thermogravimetric analysis (DTG). This analysis investigated the weight loss and heat flow associated with YBCO decomposition, providing insights into the thermal stability and potential phase transitions during the synthesis process [19, 20]. Notably, the TGA curves exhibited distinct weight loss stages at specific temperatures, while the DTG curves revealed

peaks corresponding to the maximum rate of decomposition [21] . The initial weight loss stage observed in both methods is attributed to the dehydration of adsorbed water, commencing from around 51.51 °C to 174.32 °C for YBCO-SSR and from 58.29 °C to 314.74 °C for YBCO-DM which is consistent with existing literature [22-24]. This was followed by a significant weight loss stage in the second drop, which was 0.95% for SSR at temperatures between 175.86 and 317.86 °C compared to DM which was 2.53% at temperatures between 315.78 and 727.90 °C which is attributed to the decomposition of organic residues, including the evolution of CO_2 and the breakdown of acetate molecules [21]. Notably, the DM method exhibited a slightly higher weight loss (around 3.53%) compared with the SSR method (0.95%) in the third stage, likely due to its enhanced effectiveness in decomposing organic matter.

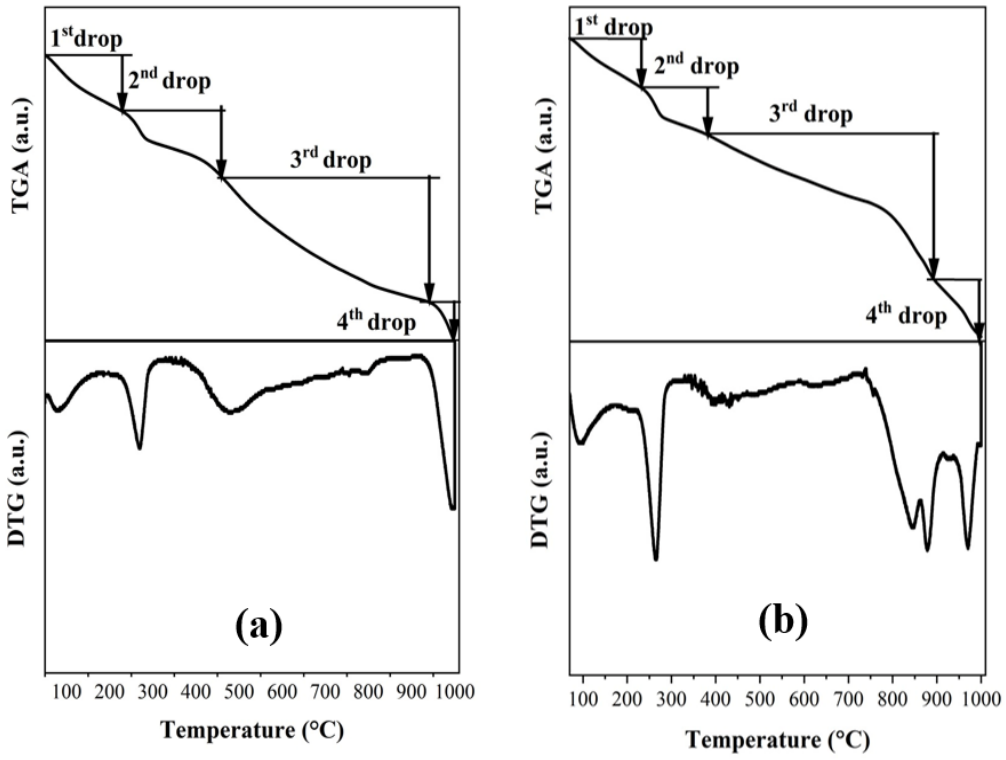

Figure 1. Thermogravimetric (TGA/DTG) Curves of the samples of (YBCO-SSR and YBCO-DM); (a) Prepared via Solid-State Reaction (YBCO-SSR) and (b) Prepared by novel modified thermal decomposition (YBCO-DM)

Additionally, the pre-calcination phase in the DM method likely removed unwanted impurities, resulting in more complete decomposition than the SSR method, as observed by the higher total weight loss in DM compared to SSR. DTG analysis further confirmed this by revealing a larger peak at around 990 °C for the SSR method, indicating incomplete decomposition of specific components compared to the DM method [25]. Finally, the negligible weight loss at higher temperatures observed in the TGA curves indicates the successful transition of the precursor materials into their respective pure metal oxides. This critical phase marks the formation of YBCO single crystals, commencing around 874.09 °C for DM and 850 °C for the SSR method [18, 25, 26]. Notably, the synthesis processes culminated in the production of orthorhombic structured YBCO single crystals once the temperature surpasses 960 °C. Such TGA/DTG analytical results are instrumental in refining the YBCO synthesis process, as they provide essential information about the material's

thermal stability and phase transition behavior, allowing for the evaluation and enhancement of the synthesis techniques employed.

XRD Analysis

Figure 2 shows the XRD patterns of the YBCO samples. XRD data analysis revealed both samples to be predominantly composed of the YBCO phase with an orthorhombic crystal structure (ICSD: 98-002-4717). Notably, no orthorhombic-tetragonal phase transition was observed. Minor traces of a secondary (Y-211) phase (ICSD: 98-002-4901) were present in both samples, while the YBCO-SSR sample additionally presented a faint secondary phase identified as (CuO) (98-008-7540). Interestingly, the sample prepared using the modified thermal decomposition (YBCO-DM) exhibited a higher volume fraction of the YBCO phase than the sample prepared via solid-state reaction (YBCO-SSR). In both samples, the most intense peak, at $2\theta \approx 32.8095°$, corresponded to the (103) Miller indices of the YBCO phase. As shown in Table 1, the YBCO-DM sample displayed more significant lattice parameters (a, b, and c) and crystallite size compared to the YBCO-SSR sample, suggesting an influence of the crystal structure on these factors. Consequently, the YBCO-DM sample also exhibited a larger unit cell volume [27]. It is noteworthy that the observed highest orthorhombicity value in YBCO-SSR, likely associated with its specific oxygen content (6.84), contrasts with the lower value observed in YBCO-DM, calculated oxygen content (6.82) using the equation $7\text{-}\delta = 75.25 - 5.86c$, where ($c$) represents the lattice parameter on the y-axis in the YBCO system) [28, 29]. While the YBCO-DM sample exhibited a slightly lower oxygen content compared to YBCO-SSR, the difference is relatively small ($\Delta\delta \approx 0.03$). Therefore, it is unlikely that this minor variation in oxygen content alone can account for the significant differences observed in the microstructure and superconducting transition temperature T_c between the two samples. The more prominent factors influencing the microstructural and superconducting properties are likely the synthesis method.

The DM method employs metal acetates as precursors, promoting a more homogeneous elemental distribution during synthesis. This process results in a denser and more uniform microstructure, as confirmed by FESEM analysis, enhancing oxygen ordering along the b-axis in the Cu-O-Cu chains and increasing twin density [30]. These factors contribute to better flux pinning and stronger intergranular coupling in the YBCO-DM sample, leading to a higher onset of T_c and a sharper superconducting transition compared to the YBCO-SSR sample. Thus, while oxygen content is an important factor, it is the synthesis conditions and material homogeneity that more critically influence the superconducting properties of the samples.

Table 1. Lattice parameters, orthorhombicity, unit cell volume, and volume fraction of the YBCO- SSR and YBCO-DM samples

	Lattice Parameters			Orthorhombicity	Volume	Vol. Fraction %			Cryst. Size
Sample	a /Å	b /Å	c /Å	$\frac{(b-a)}{(a+b)}$	/Å^3	YBCO	Y211	CuO	/Å
YBCO-SSR	3.8210	3.8846	11.681	0.00825	173.38	78.2	7.7	13	920
YBCO-DM	3.8215	3.8848	11.685	0.00821	173.44	98.6	1.4	-	1062

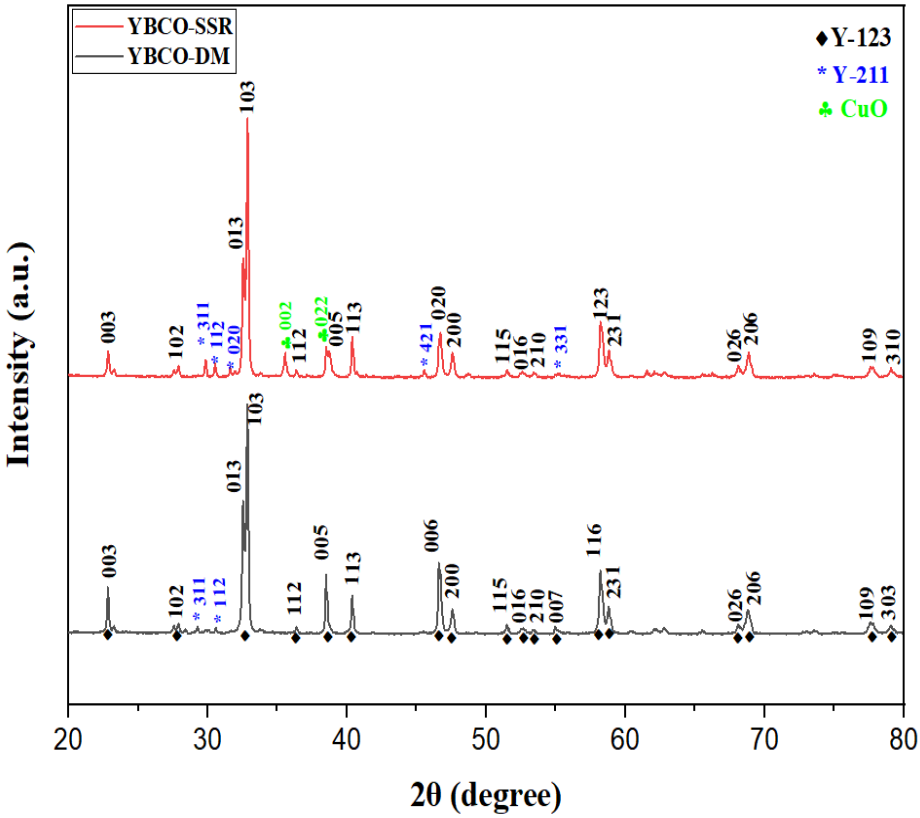

Figure 2. X-ray diffraction patterns of the samples of (YBCO-SSR and YBCO-DM) were prepared via solid-state reaction and novel modified thermal decomposition (DM)

Scanning Electron Microscopy and Elemental Analysis

Figures 3 show FESEM images of samples synthesized via the traditional solid-state reaction (YBCO-SSR) and those from an innovative modified thermal decomposition method (YBCO-DM). We used ImageJ software to quantify the average grain size by analyzing approximately 100 grains across both dimensions in each image (Figure 4 and Table 2). Figure 5 depicts the distribution of grain sizes for samples prepared using the modified thermal decomposition (DM) and solid-state reaction (SSR) methods[31, 32]. Both samples exhibit irregular structures, but YBCO-DM displays a noticeably denser packing with a smaller average grain size compared to YBCO-SSR [8]. This observation suggests that the modified thermal decomposition process offers a distinct advantage in controlling YBCO grain size. The denser packing observed in YBCO-DM is likely attributed to enhanced interconnectivity and grain rearrangement during its synthesis, promoting closely packed structures with potentially improved intergranular transport currents[8, 21]. Additionally, the smaller grains in YBCO-DM are expected to fill intergranular pores effectively, effectively linking and enhancing grain connectivity [33]. Thus, benefiting by linking the grains and enhancing the grain connectivity.

These grains become tightly packed together and improve the electron transportation between the grains [4]. Consequently, the DM method likely contributes to a denser and more compact grain structure, potentially enhancing the critical temperature (T_c) [6]. Figure 6(a-b) presents Energy-Dispersive X-ray Spectroscopy (EDX) spectra for both YBCO samples. These analyses confirm the successful formation of the YBCO phase in each sample, evidenced by the presence of the expected Y, Ba, Cu, and O elements [34]. While

the overall elemental composition appears similar, closer examination may reveal minor discrepancies in peak intensities or elemental distribution across the maps.

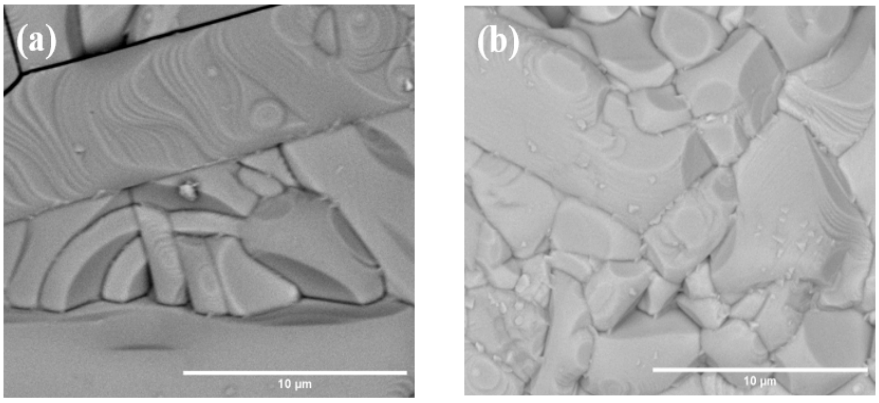

Figure 3. FESEM images at 10,000x magnification of YBCO bulk superconductors prepared by (a) solid-state reaction (YBCO-SSR) and (b) modified thermal decomposition (YBCO-DM)

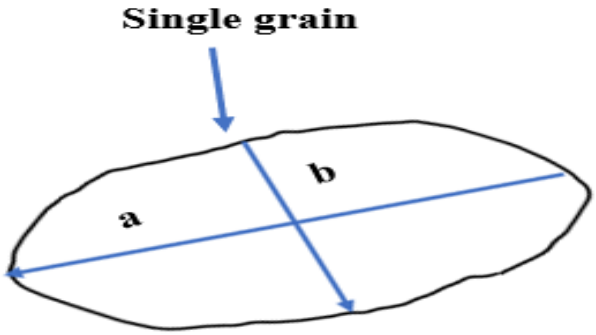

Figure 4. Schematic diagram depicting the dimensions used to measure the average grain size

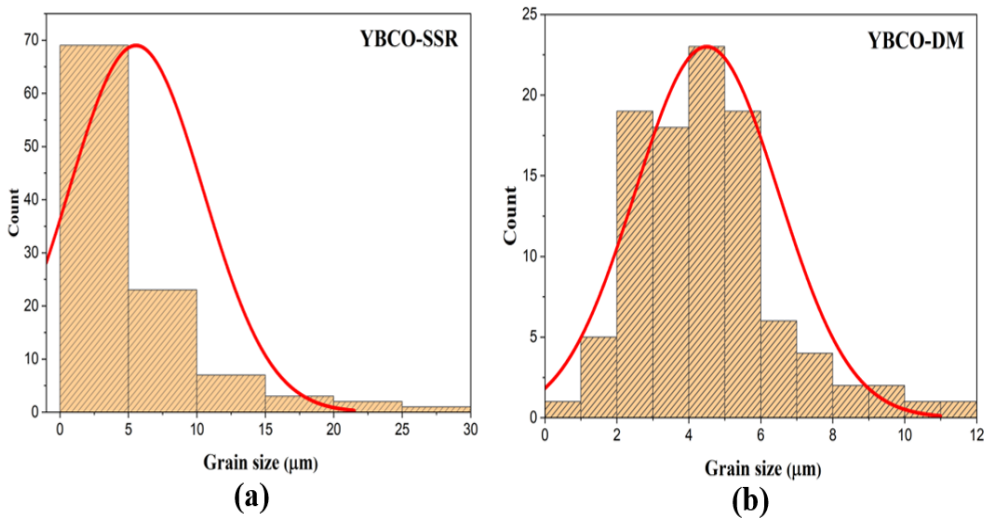

Figure 5. Distribution of the average grain size of YBCO synthesized via the (a) solid-state reaction (YBCO-SSR) and (b) modified thermal decomposition (YBCO-DM) methods

Elemental mapping was conducted to verify the homogeneity of the materials and the even distribution of elements within the samples as shown in (Figures 7(a) and 7(b) [31]. The maps for the YBCO-DM sample, in particular, indicate a more uniform distribution of yttrium, barium, copper, and oxygen compared to the YBCO-SSR sample, implying a more consistent stoichiometry and the possible reduction of unfavorable secondary phases. These maps are critical for confirming the uniform distribution of the constituent elements, which is essential for the consistency of the superconducting properties across the entire sample [35]. This observation could be attributed to the inherent advantages of the DM technique, which utilizes metal acetates as precursors and employs a precisely controlled thermal profile [36]. Such improved homogeneity may potentially enhance the electrical superconducting properties of the YBCO-DM material, warranting further investigation through relevant electrical and transport characterization techniques.

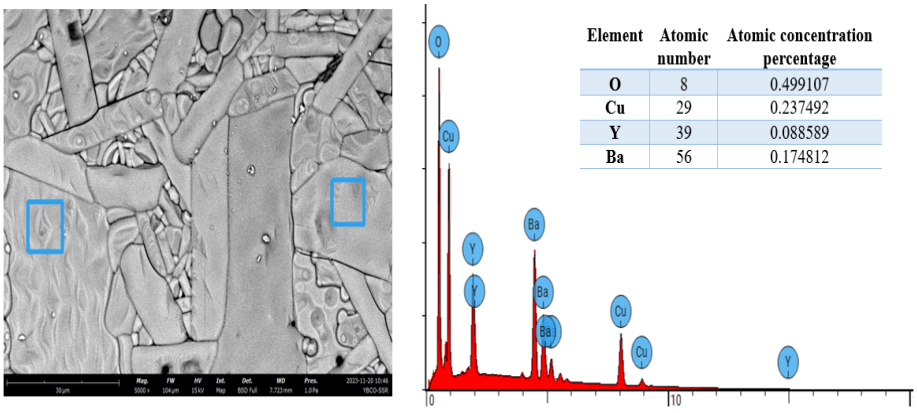

Element	Atomic number	Atomic concentration percentage
O	8	0.499107
Cu	29	0.237492
Y	39	0.088589
Ba	56	0.174812

(a)

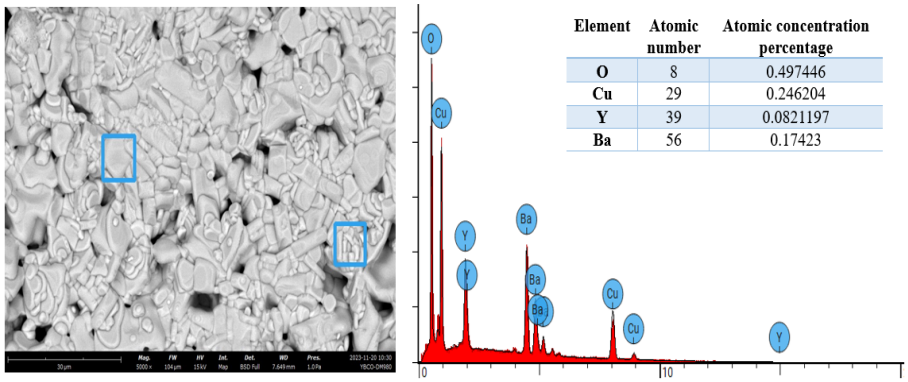

Element	Atomic number	Atomic concentration percentage
O	8	0.497446
Cu	29	0.246204
Y	39	0.0821197
Ba	56	0.17423

(b)

Figure 6. EDX spectra and elemental maps of (a) YBCO-SSR and (b) YBCO-DM

Table 2. Average grain size, *D* for both samples

Sample	Average Grain Size (*D*) /µm
YBCO-SSR	5.55 ± 0.44
YBCO-DM	4.50 ± 0.20

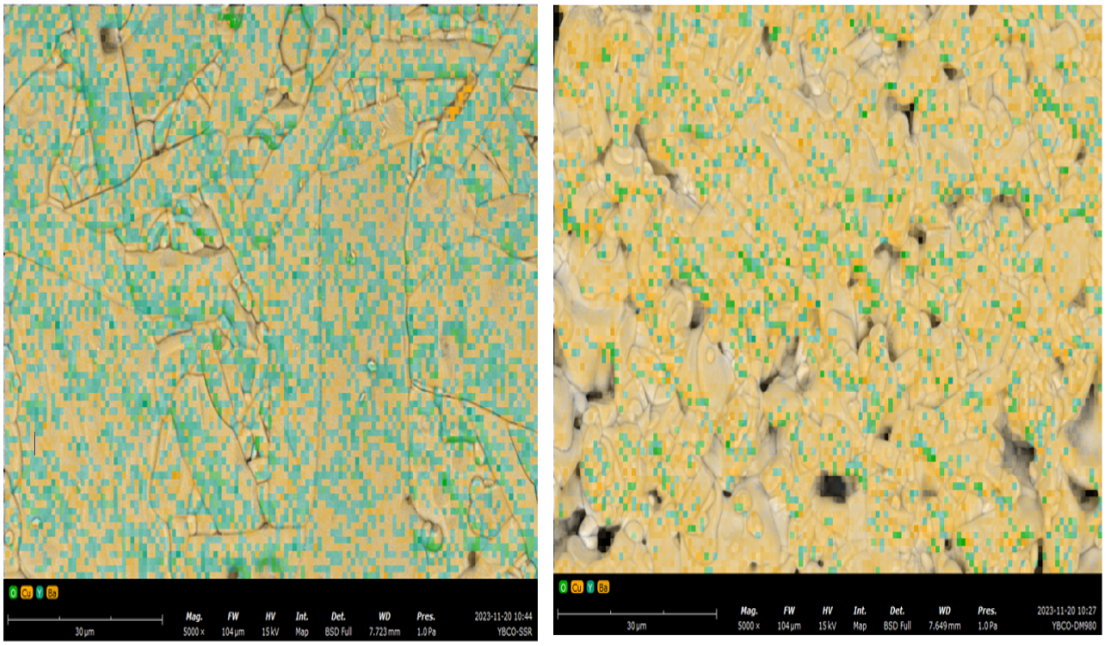

Figure 7. Elemental distribution in YBCO superconductors prepared using the (a) solid-state reaction (SSR) and (b) modified thermal decomposition (DM) methods

Electrical Resistivity Measurements

Figure 8(a) illustrates the normalized resistivity as a function of temperature for the YBCO-SSR and YBCO-DM samples. Resistivity measurements were measured using the standard four-point probe technique within a temperature range of 30 to 300 K [37]. Figure 8(b) focuses on the critical temperatures ($T_{c\text{-}onset}$ and $T_{c\text{-}zero}$) identifiable by the dρ/dT analysis, enhancing the transition's visibility and allowing for precise T_c determination. $T_{c\text{-}onset}$ is identified at the temperature where the second derivative of the resistance with respect to temperature deviates from the linear graph, indicating the start of the superconducting transition. $T_{c\text{-}zero}$ is determined at the point where resistance drops to zero, marking complete transition to the superconducting state (Table 3). Both samples exhibit a nearly linear decrease in resistivity as they cool from room temperature to the onset of the superconducting transition. This observed single-step transition in both samples indicates good grain connectivity and the prevalence of the YBCO phase, as reported in reference [38]. The width of the resistive transition temperature interval, denoted as ΔT_c, is depicted in Figure 9 [32]. The difference in ΔT_c between the two samples indicates that the DM technique effectively controls the microstructure of YBCO ceramics [11]. Notably, the significantly lower ΔT_c observed in YBCO-DM points towards a more homogeneous and well-ordered material. The enhanced homogeneity and improved intergranular connectivity observed in the YBCO-DM sample can be attributed to the superior solubility and reactivity of metal acetates, coupled with the precise control of temperature and duration during the pre-calcination and sintering steps [12]. These factors promote a highly ordered and well-connected microstructure, facilitating an efficient charge carrier transport and, ultimately leading to a sharper resistive transition and narrower ΔT_c [20]. This suggests that the DM-processed sample possesses an optimized microstructure with minimized grain boundaries and enhanced grain connectivity, ultimately contributing to superior superconducting properties [31]. The novel thermal decomposition method significantly influences the

transition width (ΔT_c) and has a pronounced impact on the sample's macrostructure and critical temperature (T_c). This finding, alongside the previously mentioned XRD analysis, suggests that the high percentage of secondary phases in the solid-state reaction sample likely detrimentally affects the critical temperature [5,39]. Conversely, it is possible to enhance the critical current density, J_c [32, 40].

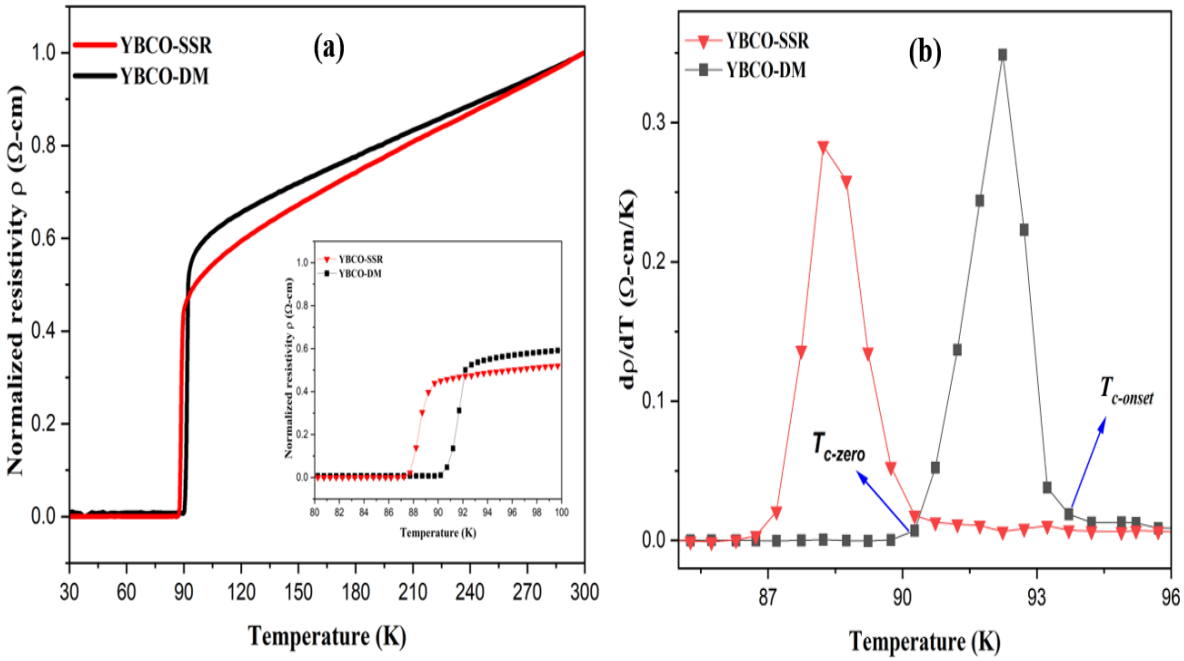

Figure 8. (a) Normalized resistivity versus temperature curve of YBCO-SSR and YBCO-DM samples and (b) derivative of resistivity against temperature of both samples

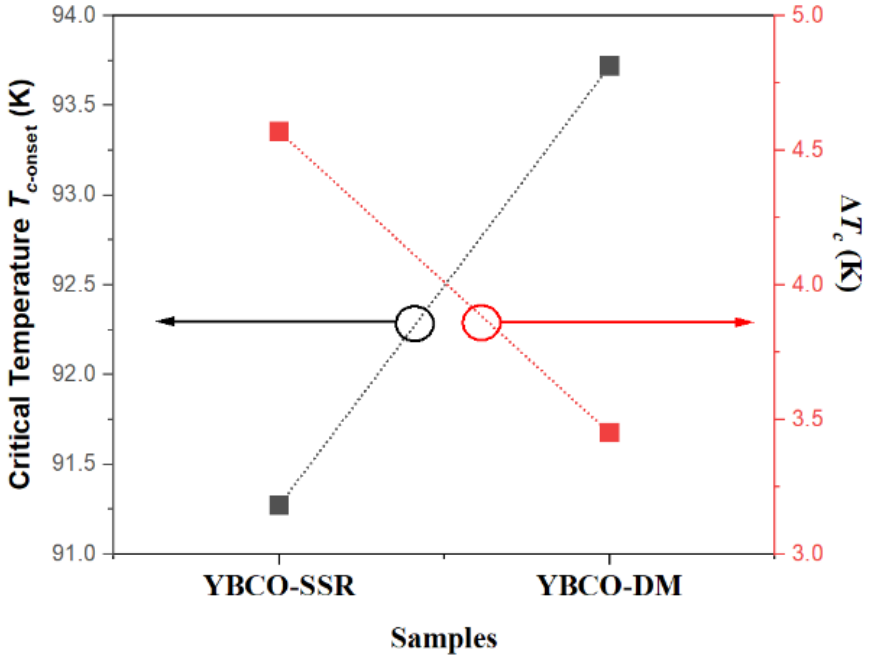

Figure 9. The relationship between $T_{c\text{-}onset}$ and ΔT_c of both samples

Table 3. $T_{c\text{-}onset}$, $T_{c\text{-}zero}$, and ΔT_c of both samples

Sample	$T_{c\text{-}onset}$ / K	$T_{c\text{-}zero}$ / K	ΔT_c / K
YBCO-SSR	91.3	86.7	4.6
YBCO-DM	93.7	90.3	3.5

CONCLUSIONS

This study presents a compelling comparison between the established solid-state reaction (SSR) technique and an innovative modified thermal decomposition (DM) method for synthesizing high-performance $YBa_2Cu_3O_{7-\delta}$ (YBCO) superconductors. Through meticulous X-ray diffraction (XRD) analysis, we verified the formation of the principal YBCO phase in specimens synthesized by SSR and DM methods, despite secondary phases such as Y211 and CuO. Significantly, field emission scanning electron microscopy (FESEM) examination exposed pronounced microstructural disparities, with the DM method yielding specimens characterized by finer average grain size and a markedly denser packing than those prepared via SSR, suggesting a more uniform and compact microstructure. This microstructural refinement, especially the smoother grain boundaries observed in the YBCO-DM specimens, is proposed to enhance supercurrent flow, potentially elevating the critical temperature (T_c). Furthermore, our findings indicate that the YBCO synthesized through the DM technique not only displayed a higher superconducting transition temperature ($T_{c\text{-}onset}$ and $T_{c\text{-}zero}$) but also exhibited a sharper transition curve and transition temperature width (ΔT_c), indicative of superior superconductivity. These notable improvements are attributed to two critical factors: the strategic use of acetate as a single starting material, promoting a more orderly elemental distribution within the YBCO matrix, and the microstructural optimization through reduced grain size and denser packing. These modifications are believed to enhance intergranular transport currents, improve grain connectivity, and develop a more compact grain structure, collectively contributing to an increased critical temperature (T_c).

The DM technique presents a superior approach for synthesizing YBCO superconductors, with notable improvements in the superconducting properties and a novel solution to challenges in material fabrication. This study highlights the need for further research to optimize the DM method, which could lead to significant technological advancements in fields ranging from energy to medical imaging. By addressing unique challenges and suggesting new research avenues, this work sets the stage for a new era of enhanced YBCO superconductors, promising significant impacts on superconductivity applications and technology.

ACKNOWLEDGEMENTS

This research was supported by the Ministry of Higher Education, Malaysia under FRGS Grant No. FRGS/1/2020/STG07/UPM/02/4 and was partly supported by the Japan Science and Technology Agency (JST) for advanced Project Based Learning (aPBL), Shibaura Institute of Technology (SIT) under Top Global University Project, designed by the Ministry of Education, Culture, Sports, and Science & Technology of Japan.

REFERENCES

[1] M.K.Wu, J.R. Ashburn, C.J. Torng, P.H. Hor, R.L. Meng, L. Gao, Z.J. Huang, Y. Wang, C.W. Chu (1987). Superconductivity at 93 K in a new mixed-phase Y-Ba-Cu-O compound system at ambient pressure, *Physical Review Letters* **58**(9), 908.

[2] C. Chu, 1987. Superconductivity above 90 K, *Proc. Natl. Acad. Sci. U S A*. **84**(14), 4681.

[3] L. Pathak, S.K. Mishra (2005). A review on the synthesis of Y–Ba–Cu-oxide powder, *Superconductor Science and Technology* **18**, R67.

[4] N.A.C. Dzul-Kifli, M.M.A. Kechik, H. Baqiah, A.H. Shaari, K.P. Lim, S.K. Chen, S.I.A. Sukor, M.K. Shabdin, M.K.A. Karim, K.K.M. Shariff (2022). Superconducting properties of $YBa_2Cu_3O_{7-\delta}$ with a multiferroic addition synthesized by a capping agent-aided thermal treatment method, *Nanomaterials* **12,** 3958.

[5] S. Miryala (2020). Prospects of superconducting magnet technology in the medical field: A new paradigm on the horizon? *Superconductivity: From Materials Science to Practical Applications,* Switzerland: Springer Nature p. 353.

[6] M.M. Dihom, A.H. Shaari, H. Baqiah, N.M. Al-Hada, S.K. Chen, R.b.a.S. Azis, M.M.A. Kechik, R. Abd-Shukor (2017). Effects of calcination temperature on microstructure and superconducting properties of Y123 ceramic prepared using thermal treatment method, *Solid State Phenomena* **268,** 325.

[7] M. Ochsenkühn-Petropoulou, R. Argyropoulou, P. Tarantilis, E. Kokkinos, K. Ochsenkühn, G. Parissakis (2002). Comparison of the oxalate co-precipitation and the solid state reaction methods for the production of high temperature superconducting powders and coatings, *Journal of Materials Processing Technology,* **127**(1), 122.

[8] N. Mohd Hapipi, A.H. Shaari, M.M.A. Kechik, K.B. Tan, R. Abd-Shukor, N.R. Mohd Suib, S.K. Chen (2017). Effect of heat treatment condition on the phase formation of $YBa_2Cu_3O_{7-\delta}$ superconductor, *Solid State Phenomena* **268,** 305.

[9] T. Chin, T. Huang, W. Lin, N. Wu, Y. Chou, T. Wu, P. Wu, H. Yen (1987). The formation of Y-Ba-Cu-O phases during solid state reaction, *MRS Proceedings* **99**, 261.

[10] O. Ozturk, R. Arebat, A. Nefrow, F. Bulut, G. Guducu, E. Asikuzun, S. Celik (2019). Investigation of structural, superconducting and mechanical properties of Co/Cu substituted YBCO-358 ceramic composites, *Journal of Materials Science: Materials in Electronics* **30**, 7400-9.

[11] R. Al-Gaashani, B. Aïssa, M.A. Hossain, S. Radiman (2019). Catalyst-free synthesis of ZnO-CuO-$ZnFe_2O_4$ nanocomposites by a rapid one-step thermal decomposition approach, *Materials Science in Semiconductor Processing* **90**, 41.

[12] R. Al-Gaashani, S. Radiman, N. Tabet, A.R. Daud (2011). Synthesis and optical properties of CuO nanostructures obtained via a novel thermal decomposition method, *Journal of Alloys and Compounds* **509**, 8761.

[13] N.N. Mohd Yusuf, M.M. Awang Kechik, H. Baqiah, C. Soo Kien, L. Kean Pah, A.H. Shaari, W.N.W. Wan Jusoh, S.I. Abd Sukor, M. Mousa Dihom, Z.A. Talib (2018). Structural and superconducting properties of thermal treatment-synthesised bulk $YBa_2Cu_3O_{7-\delta}$ superconductor: Effect of addition of SnO_2 nanoparticles, *Materials* **12**, 92.

[14] N.M. Hapipi, S.K. Chen, A.H. Shaari, M.M.A. Kechik, K.B. Tan, and K.P. Lim (2018). Superconductivity of Y_2O_3 and $BaZrO_3$ nanoparticles co-added YBa_2 Cu_3 $O_{7-\delta}$ bulks prepared using co-precipitation method, *Journal of Materials Science: Materials in Electronics* **29**, 18684.

[15] X. Zhang, D. Zhang, X. Ni, J. Song, H. Zheng (2008). Synthesis and electrochemical properties of different sizes of the CuO particles, *Journal of Nanoparticle Research* **10,** 839.
[16] G. Peleckis, K. Tõnsuaadu, T. Baubonyte, A. Kareiva (2002). Sol–gel chemistry approach in the preparation of precursors for the substituted superconducting oxides, *Journal of Non-Crystalline Solids* **311(**3), 250.
[17] B. Glowacki, M. Mosiadz (2009). The role of sol gel processing in the development of high-temperature superconductors for AC applications, *Journal of Sol-Gel Science and Technology* **51**, 335-47.
[18] Songchol Hong, Un Yong Paek, Song Ho Kim, Yang Qi, Xingming Zhao (2022) Formation of YBCO superconducting phase, *International Conference on Environmental Science and Green Energy (ICESGE)* 9-11 Dec., pg. 238.
[19] L. M. Yeoh, R. Abd-Shukor (2008). The study on various wet chemistry techniques on $YBa_2Cu_3O_{7-\delta}$ superconducting oxides powder preparation, *Journal of Non-Crystalline Solids* **354(**34), 4043.
[20] S. Hong, R.S. Kim, Y. Qi, X. Zhao, S.H. Kim, Y.G. Ryu (2023). Thermal decomposition of precursor of $YBa_2Cu_3O_{7-\delta}$ superconducting layer *Reaction Kinetics, Mechanisms and Catalysis* **136**(5), 2801.
[21] A.N. Kamarudin, M.M. Awang Kechik, M. Miryala, S. Pinmangkorn, M. Murakami, S.K. Chen, H. Baqiah, A. Ramli, K.P. Lim, A.H. Shaari (2021). Microstructural, phase formation, and superconducting properties of bulk $YBa_2Cu_3O_y$ superconductors grown by infiltration growth process utilizing the $YBa_2Cu_3O_{y+}$ $ErBa_2Cu_3O_{y+}$ $Ba_3Cu_5O_8$ as a liquid source, *Coating* **11**(4), 377.
[22] P. Melnikov, V. Nascimento, L. Consolo, A. Silva (2013). Mechanism of thermal decomposition of yttrium nitrate hexahydrate, Y $(NO_3)3{\cdot}6H_2O$ and modeling of intermediate oxynitrates, *Journal of Thermal Analysis and Calorimetry* **111**, 115-9.
[23] T.T. Thuy, S. Hoste, G. Herman, K. De Buysser, P. Lommens, J. Feys, D. Vandeput, I. Van Driessche (2009). Sol–gel chemistry of an aqueous precursor solution for YBCO thin films, *Journal of Sol-Gel Science and Technology* **52**, 124.
[24] W. Zhao, Y. Shi, M. Radušovská, A.R. Dennis, J.H. Durrell, P. Diko, D.A. Cardwell (2016). Comparison of the effects of platinum and CeO_2 on the properties of single grain, Sm–Ba–Cu–O bulk superconductors, *Superconductor Science and Technology* **29**(12), 125002.
[25] J. Fei, H. Zhang, W. Wenzhang, L. Xiang, C. Qingming (2017). Improvement in structure and superconductivity of $YBa_2Cu_3O_{6+\delta}$ ceramics superconductors by optimizing sintering processing, *Journal of Rare Earths* **35**(1), 85.
[26] M. Wahid, Z. Zainal, I. Hamadneh, K. Tan, S. Halim, A. Rosli, E. Alaghbari, M. Nazarudin, E. Kadri (2012). Phase formation of $REBa_2Cu_3O_{7-\delta}$ (RE: $Y_{0.5}Gd_{0.5}$, $Y_{0.5}Nd_{0.5}$, $Nd_{0.5}Gd_{0.5}$) superconductors from nanopowders synthesised via co-precipitation, *Ceramics International* **38**(2), 1187.
[27] M.A. Kechik, P. Mikheenko, A. Sarkar, V.-S. Dang, N.H. Babu, D. Cardwell, J. Abell, A. Crisan (2009). Artificial pinning centres in $YBa_2Cu_3O_{7-\delta}$ thin films by $Gd_2Ba_4CuWO_y$ nanophase inclusions, *Superconductor Science and Technology* **22**(3), 034020.
[28] A. Bahboh, A.H. Shaari, H. Baqiah, C.S. Kien, M.M.A. Kechik, M.H. Wahid, R. Abd-Shukor, Z.A. Talib (2019). Effects of $HoMnO_3$ nanoparticles addition on microstructural, superconducting and dielectric properties of $YBa_2Cu_3O_{7-}$, *Ceramics International* **45**(11) 13732.
[29] P. Benzi, E. Bottizzo, N. Rizzi (2004). Oxygen determination from cell dimensions in YBCO superconductors, *Journal of Crystal Growth* **269**(2-4), 625.

[30] T.G. Holesinger, L. Civale, B. Maiorov, D.M. Feldmann, J.Y. Coulter, D.J. Miller, V.A. Maroni, Z. Chen, D.C. Larbalestier, R. Feenstra (2008). Progress in nanoengineered microstructures for tunable high-current, high-temperature superconducting wires, *Advanced Materials* **20**(3), 391.

[31] S.N. Abdullah, M.M.A. Kechik, A.N. Kamarudin, Z.A. Talib, H. Baqiah, C.S. Kien, L.K. Pah, M.K. Abdul Karim, M.K. Shabdin, A.H. Shaari (2023). Microstructure and superconducting properties of Bi-2223 synthesized via co-precipitation method: Effects of graphene nanoparticle addition, *Nanomaterials* **13**(15), 2197.

[32] N.A. Khalid, M.M.A. Kechik, N.A. Baharuddin, C.S. Kien, H. Baqiah, N.N.M. Yusuf, A.H. Shaari, A. Hashim, Z.A. Talib (2018). Impact of carbon nanotubes addition on transport and superconducting properties of $YBa_2Cu_3O_{7-\delta}$ ceramics, *Ceramics International* **44**(8), 9568.

[33] M.M. Dihom, A.H. Shaari, H. Baqiah, C.S. Kien, R.S. Azis, R. Abd-Shukor, N.M. Al-Hada, M.M.A. Kechik, Z.A. Talib (2019). Calcium-substituted $Y_3Ba_5Cu_8O_{18}$ ceramics synthesized via thermal treatment method: structural and superconducting properties, *Journal of Superconductivity and Novel Magnetism* **32**, 1875.

[34] A.R. Hamoudi, A. May, A. Henniche, J.-H. Ouyang, A. Guillet (2021). A comparative study of (Ce) and (Gd) doping influence on the superconducting properties of YBCO ceramics, *Ceramics International* **47**(18), 25314.

[35] H. Baqiah, S.A. Halim, S.K. Chen, K.P. Lim, M.M. Awang Kechik (2016). Effects of rare earth nanoparticles (M = Sm_2O_3, Ho_2O_3, Nd_2O_3)addition on the microstructure and superconducting transition of $Bi_{1.6}Pb_{0.4}Sr_2Ca_2Cu_3O_{10+\delta}$ ceramics. *Sains Malays.* **45**(4), 643.

[36] A.N. Kamarudin, M.M. Awang Kechik, S.N. Abdullah, H. Baqiah, S.K. Chen, M.K. Abdul Karim, A. Ramli, K.P. Lim, A.H. Shaari, M. Miryala (2022). Effect of graphene nanoparticles addition on superconductivity of $YBa_2Cu_3O_{7-\delta}$ synthesized via the thermal treatment method, *Coatings* **12**(1), 91.

[37] F. Barood, M.M.A. Kechik, T.S. Tee, C.S. Kien, L.K. Pah, K.J. Hong, A.H. Shaari, H. Baqiah, M.K.A. Karim, M.K. Shabdin (2023). Orthorhombic $YBa_2Cu_3O_{7-\delta}$ superconductor with TiO_2 nanoparticle addition: crystal structure, electric resistivity, and AC susceptibility, *Coatings* **13**(6), 1093.

[38] I. Hamadneh, A. Rosli, R. Abd-Shukor, N. Suib, S. Yahya (2008). Superconductivity of $REBa_2Cu_3O_{7-\delta}$ (RE= Y, Dy, Er) ceramic synthesized via coprecipitation method, *Journal of Physics: Conference Series* **97**, 012063.

[39] D. Gokhfeld, S. Semenov, D. Balaev, I. Yakimov, A. Dubrovskiy, K.Y. Terentyev, A. Freydman, A. Krasikov, M. Petrov (2017). Establishing of peak effect in YBCO by Nd substitution, *Journal of Magnetism and Magnetic Material* **440**, 127.

[40] B. Sahoo, K.L. Routray, D. Samal, D. Behera (2019). Effect of artificial pinning centers on YBCO high temperature superconductor through substitution of graphene nano-platelets, *Materials Chemistry and Physics* **223**, 784.